

# Epithelial–Mesenchymal Transition Enhances Response to Oncolytic Herpesviral Therapy Through Nectin-1

Chun-Hao Chen,<sup>1</sup> Wei-Yi Chen,<sup>2</sup> Shu-Fu Lin,<sup>1,3</sup> and Richard J. Wong<sup>1</sup>

## Abstract

Cancers exhibiting epithelial–mesenchymal transition (EMT) are associated with aggressive behavior and increased metastatic potential. Therapies that are able to target EMT would have significant clinical value. Nectin-1 is a cell surface herpes simplex virus type 1 (HSV-1) receptor that also forms a component of intercellular adherens junctions, which are typically disrupted in EMT. To explore relationships between HSV-1 sensitivity and EMT, we generated cell lines with a stable EMT phenotype from human follicular thyroid cancer (WRO82-1) through E-cadherin silencing with short hairpin RNA (shEcadWRO). HSV-1 viral attachment and gene expression were both enhanced in shEcadWRO as compared with shControl. Immunoblotting and immunostaining revealed enhanced nectin-1 expression by shEcadWRO. Receptor-blocking assays demonstrated that increased herpesviral entry into shEcadWRO as compared with shControl was mediated predominantly through nectin-1. Colocalization of green fluorescent protein-tagged HSV-1 and tdTomato-tagged nectin-1 confirmed an increase in viral attachment to nectin-1 in shEcadWRO. Cell viability assays demonstrated increased susceptibility of shEcadWRO to HSV-1 oncolysis, and a murine flank tumor model showed significantly enhanced regression of shEcadWRO tumors in response to oncolytic HSV-1 as compared with control tumors. A separate model of EMT induction through transforming growth factor- $\beta$  stimulation confirmed enhanced HSV-1 susceptibility in Panc1 cells. These results demonstrate that the process of EMT leads to increased herpesviral susceptibility through enhanced cell surface nectin-1 expression, suggesting that cancers exhibiting EMT may be naturally sensitive targets for herpesviral therapy.

## Introduction

**E**PITHELIAL–MESENCHYMAL TRANSITION (EMT) is a fundamental developmental and oncogenic process through which cells shift from an epithelial to a mesenchymal phenotype, express mesenchymal markers, lose cell polarity, lose cell–cell adherens junctions, and lose the expression of epithelial markers such as E-cadherin (Kalluri and Weinberg, 2009; Thiery *et al.*, 2009). Cells undergoing EMT typically gain migratory ability as a result of this transition, and this process has been found to be important during both organ development and in cancer progression. Cancer cells that have undergone EMT are generally more able to invade locally and metastasize to lymph nodes and to distant sites (Fidler, 2003; Thompson *et al.*, 2005; Hugo *et al.*, 2007; Polyak and Weinberg, 2009). The acquisition of an EMT phenotype has also been associated with resistance to che-

motherapy and radiation therapy, and is considered to be reflective of aggressive tumor behavior (Yang *et al.*, 2006; Shah *et al.*, 2007; Kurrey *et al.*, 2009).

The development of novel therapies with novel mechanisms of activity for aggressive tumor subtypes, such as cancers exhibiting EMT, is critical to improve clinical outcomes. Oncolytic herpes simplex viral (HSV) therapy harnesses the natural ability of a replication-competent, herpesvirus to infect, replicate within, and lyse cancer cells. Most of these viruses have been genetically attenuated for enhanced safety, and yet retain potent antitumoral effects against solid tumors in animal models (Mineta *et al.*, 1995; Coukos *et al.*, 2000; Wong *et al.*, 2001b; Peng *et al.*, 2002; Lin *et al.*, 2008). We have described the construction of NV1023 (Bennett *et al.*, 2001; Wong *et al.*, 2001b, 2002, 2004; Yu *et al.*, 2004; Gil *et al.*, 2007; Reid *et al.*, 2008) and NV1066 (Wong *et al.*, 2001a, 2002; Stanziale *et al.*, 2004;

<sup>1</sup>Department of Surgery, Memorial Sloan-Kettering Cancer Center, New York, NY 10021.

<sup>2</sup>Laboratory of Biochemistry and Molecular Biology, Rockefeller University, New York, NY 10021.

<sup>3</sup>Department of Internal Medicine, Chang Gung Memorial Hospital, Chang Gung University, Taoyuan, 33305 Taiwan, Republic of China. This work was performed in New York, NY.

Eisenberg *et al.*, 2005), which are replication-competent, attenuated HSV-1 with significant oncolytic effects against a variety of human malignancies. Our group found that herpesviral efficacy in treating cancers may be dependent on the relative expression of a herpesviral receptor, nectin-1, by cancer cells (Huang *et al.*, 2007; Yu *et al.*, 2007a,b, 2008). Nectin-1 is a receptor for viral envelope glycoprotein D expressed by HSV-1. Nectin-1 also forms an important component of intercellular adherens junctions, along with E-cadherin.

Interestingly, the disruption of adherens junctions and cell-cell contacts between cancer cells through calcium depletion liberates nectin-1 that is normally engaged in the adherens junctions (Yoon and Spear, 2002). Released nectin-1 is able to serve as a functional receptor for oncolytic herpesviral therapy (Yu *et al.*, 2007b), increasing therapeutic efficacy. Because EMT ultimately results in a similar disruption of adherens junctions, although through a different mechanism, we hypothesized that cells undergoing EMT might demonstrate an altered sensitivity to oncolytic HSV-1 therapy. Cancers that have undergone EMT are typically more aggressive tumors with increased metastatic potential, posing a clinical challenge.

Here we demonstrate that the induction of EMT, through the repression of E-cadherin or transforming growth factor (TGF)- $\beta$  stimulation, increases cancer cell nectin-1 expression, permitting enhanced herpesviral entry into these cells. These effects translate to enhanced cytotoxicity *in vitro* and tumor regression *in vivo* in a murine flank tumor model. These findings demonstrate that the process of EMT may naturally and significantly enhance cancer sensitivity to herpesviral therapies.

## Materials and Methods

### Cell culture

WRO82-1, a human thyroid follicular carcinoma, was maintained in RPMI supplemented with nonessential amino acids (NEAAs), 2 mM L-glutamine, 1 mM sodium pyruvate, sodium bicarbonate (1.5 g/liter), 10% fetal calf serum (FCS), and 1% penicillin and streptomycin. Parental, unmodified WRO82-1 is termed WRO in this study. Panc-1, a human pancreatic adenocarcinoma cell line, was grown in DME HG (Dulbecco's modified Eagle's medium-high glucose) supplemented with 1 mM sodium pyruvate, sodium bicarbonate (1.5 g/liter), 10% FCS, and 1% penicillin and streptomycin. Cells were incubated at 37°C in 5% carbon dioxide.

### E-cadherin repression and stable cell line generation

Short hairpin RNA (shRNA) constructs targeting E-cadherin or green fluorescent protein (GFP) as a control were previously described (Onder *et al.*, 2008) (gifts from R.A. Weinberg, Whitehead Institute for Biomedical Research, Cambridge, MA) and may be used to induce EMT. Viral production and infection of cells were performed as previously described (Stewart *et al.*, 2003). Infected WRO cells were selected in puromycin (2  $\mu$ g/ml; Sigma Aldrich, St. Louis, MO) for over 2 weeks. Single cells were isolated for clonal expansion, and screened for E-cadherin depletion by Western blot. Two E-cadherin-repressed clones are termed WRO-E1 and WRO-E2. Clone WRO-C was generated by

infection of WRO, using a lentivirus expressing shRNA targeting GFP as a control.

To generate fluorescence-tagged nectin-1-expressing cells, the coding sequence of human nectin-1 was amplified by PCR from pCK454 (gift from C. Krummenacher, Department of Microbiology, University of Pennsylvania School of Dental Medicine, Philadelphia, PA) and inserted in-frame in the N terminus of tdTomato through the *NheI* and *AgeI* sites of the pEF1 $\alpha$ -tdTomato vector (Clontech, Mountain View, CA) to create pEF1 $\alpha$ -Nectin-1-tdTomato. WRO82-1 cells were transfected with pEF1 $\alpha$ -Nectin-1-tdTomato, subsequently infected with the shRNA constructs described previously, and selected in puromycin (2  $\mu$ g/ml) for over 2 weeks to obtain WRO-Nectin-1-tdTomato-C (shRNA control) and WRO-Nectin-1-tdTomato-E (shRNA targeting E-cadherin).

### Antibodies, immunofluorescence, reagents

The following antibodies were obtained commercially: E-cadherin (BD Biosciences, San Jose, CA), fibronectin (BD Biosciences); vimentin (Dako, Carpinteria, CA); actin (Santa Cruz Biotechnology, Dallas, TX); ICP27, ICP8, and glycoprotein-C (gC) (Abcam, Cambridge, MA); nectin-1 (CK8; Invitrogen, Grand Island, NY); and a second nectin-1 antibody (CK41, a generous gift from C. Krummenacher, Department of Microbiology, School of Dental Medicine, University of Pennsylvania) (Krummenacher *et al.*, 2004). For immunofluorescence staining, cells were grown on chamber slides and fixed in methanol and ethanol (1:1). Fixed cells were immunostained with the indicated primary antibodies followed by detection with Alexa Fluor 488-conjugated anti-mouse IgG secondary antibodies (Invitrogen). Images were obtained by laser scanning confocal microscopy. Human TGF- $\beta$  was purchased from R&D Systems (Minneapolis, MN).

### Viruses

HSV-1 VP-16-GFP was a gift from D.A. Leib (Department of Microbiology and Immunology, Dartmouth Medical School, Lebanon, NH) (La Boissière *et al.*, 2004), and carries GFP-tagged VP16 within infectious HSV-1 particles, making the virus directly visible by fluorescence microscopy. NV1023 is an attenuated, replication-competent HSV-1 that expresses  $\beta$ -galactosidase in the host cell after infection, whose construction has previously been described (Wong *et al.*, 2001b). NV1066 is also an attenuated, replication-competent HSV-1 that expresses a green fluorescent protein (GFP) in the host cell after infection, and its construction has also previously been described (Wong *et al.*, 2002). Both NV1023 and NV1066 were originally provided by Medigene (Planegg/Martinsried, Germany).

### Migration and invasion assays

Cells were serum-starved with 0.5% FCS overnight. Equal numbers of cells were prepared in serum-free medium and seeded in cell culture inserts for migration assays (BD Biosciences). Medium containing 10% FCS was used as a chemoattractant. After incubation for 4 hr, membranes were washed, fixed, and stained with crystal violet. The number of cells on each membrane was counted from five high-

power microscopy fields. Invasion assays were performed with Cultrex 24-well basement membrane extract (BME) cell invasion assay kits (Trevigen, Gaithersburg, MD) according to the manufacturer's protocol.

#### *Time-lapse microscopy of viral attachment*

Equal numbers of WRO-C and WRO-E1 cells were added to glass chamber slides and infected with HSV-1 VP-16-GFP at a multiplicity of infection (MOI) of 10. A confocal microscope (Zeiss, Oberkochen, Germany) was used to detect herpesviral particle attachment to cell surfaces, with images taken in predetermined fields at 5-min intervals. Similar experiments were performed with WRO-Nectin-1-tdTomato-C and WRO-Nectin-1-tdTomato-E cells at an MOI of 20. tdTomato and GFP signals were colocalized with MetaMorph image analysis software (Molecular Devices, Sunnyvale, CA).

#### *Viral entry assays*

NV1023 expresses  $\beta$ -galactosidase on infecting cells. To assess viral entry, NV1023 was added to cells at an MOI of 0.5 or 5, and the cells were then stained with 5-bromo-4-chloro-3-indolyl- $\beta$ -D-galactopyranoside (X-Gal; Sigma-Aldrich) at the indicated time points or lysed for quantitative assessment of  $\beta$ -galactosidase expression, using an enhanced  $\beta$ -galactosidase assay kit (Genlantis, San Diego, CA). GFP expression by NV1066-infected cells was observed by microscopy. For an assessment of viral entry with nectin-1 receptor blocking, cells were incubated with nectin-1 antibody (R1.302.12; Dako) at 37°C for 1 hr followed by exposure to NV1023. The expression of  $\beta$ -galactosidase was quantified as described previously.

#### *TGF- $\beta$ induction model of EMT*

As an alternative model of EMT induction, Panc-1 cells were treated with either vehicle solution (4 M HCl plus 0.1% bovine serum albumin [BSA]) or TGF- $\beta$  (10 ng/ml) (R&D Systems) to induce EMT (Ellenrieder *et al.*, 2001). For viral entry assays,  $4 \times 10^4$  cells per well were plated overnight after pretreatment with TGF- $\beta$  for 48 hr, and then exposed to NV1023 at an MOI of 5. EMT markers and nectin-1 were assessed by immunoblotting of whole cell lysates.  $\beta$ -Galactosidase expression was measured as described previously at 6 and 9 hr postinfection to measure susceptibility to viral entry.

#### *Cell proliferation, cytotoxicity, and viral proliferation assays*

Equal numbers of cells were added to 6-well plates. For proliferation studies, cells were trypsinized daily and live cells were counted in a trypan blue exclusion assay. For cytotoxicity assays, cells were exposed to NV1023 at the indicated MOI and cytotoxicity was determined with a CytoTox 96 nonradioactive cytotoxicity assay (Promega, Madison, WI). For viral proliferation assays, supernatants from the cytotoxicity assay wells were removed and diluted 10-fold serially. Dilutions were added to confluent Vero cells for 4 hr and covered with 1% agarose for 2 days. Cells were stained with neutral red solution (Sigma-Aldrich) and viral plaques were counted.

#### *Murine flank tumor therapy*

Animal procedures were approved by the Memorial Sloan-Kettering Institutional Animal Care and Use Committee. Flank tumors were established for WRO-C and WRO-E2 by subcutaneously injecting  $1 \times 10^7$  cells in 50  $\mu$ l of Matrigel (BD Biosciences) into the flanks of mice. When tumors reached approximately 60 mm<sup>3</sup> in dimension, the animals were distributed into experimental groups with equitable tumor volumes. Flank tumors underwent intratumoral injection of a single dose of NV1023 at  $1 \times 10^7$  plaque-forming units (PFU) or an equal volume of phosphate-buffered saline (PBS) as a control. Tumor dimensions were serially measured, and tumor volumes were calculated according to the formula for the volume of an ellipsoid:  $(4/3) \times \pi \times (\text{length}/2) \times (\text{width}/2)^2$ .

#### *Murine flank tumor X-Gal histochemistry and immunofluorescence*

Established WRO-C and WRO-E2 flank tumors were injected intratumorally with NV1023 ( $1 \times 10^7$  PFU). After 24 and 48 hr, animals were killed and flank tumors were excised, frozen in Tissue-Tek solution (Sakura Finetek USA, Torrance, CA), and sectioned. Slides were fixed with 1% glutaraldehyde for 5 min, washed with PBS, and stained with 5-bromo-4-chloro-3-indolyl- $\beta$ -D-galactopyranoside (X-Gal, 1 mg/ml) in an iron solution of K<sub>4</sub>Fe(CN)<sub>6</sub> (5 mmol/liter) and MgCl<sub>2</sub> (2 mmol/liter) at 37°C for 2 hr. Slides were counterstained with nuclear fast red. For immunofluorescence, slides were fixed with methanol and ethanol (1:1) and then incubated with primary antibodies to E-cadherin, nectin-1, and vimentin. After incubating with a secondary Alexa Fluor 488-conjugated anti-mouse IgG antibody, signal was detected with confocal microscopy.

## **Results**

### *Stable E-cadherin silencing induces EMT in WRO82-1*

To generate a model of EMT in human follicular thyroid cancer cells, WRO82-1 cells were infected with lentivirus carrying shRNA targeting E-cadherin or GFP as a control. Two independent E-cadherin-depleted clones were selected, termed WRO-E1 and WRO-E2. Both clones showed an EMT phenotype with cells that transitioned from a round, cuboidal epithelial phenotype to a slender, spindle-shaped, mesenchymal phenotype (Fig. 1A, top). Immunofluorescence staining confirmed the repression of E-cadherin and the expression of the mesenchymal marker vimentin in both WRO-E1 and WRO-E2 as compared with parental WRO and the control shRNA-transfected WRO-C (Fig. 1A, middle and bottom). These changes were also verified by immunoblot. WRO-E1 and WRO-E2 exhibit nearly complete knockdown of E-cadherin and show increased expression of both fibronectin and vimentin as compared with WRO or WRO-C (Fig. 1B).

We assessed whether the induction of an EMT phenotype in WRO leads to phenotypic changes in migratory and invasive ability toward 10% FCS as a chemoattractant. Transwell Boyden chamber migration assays showed an increased number of migrating WRO-E1 and WRO-E2 cells as compared with WRO and WRO-C after just 4 hr of incubation (Fig. 1C). This increase was statistically higher for WRO-E2 as compared with both WRO and WRO-C ( $p < 0.05$ , *t* test) and also for WRO-E1 as compared with WRO ( $p < 0.05$ ,



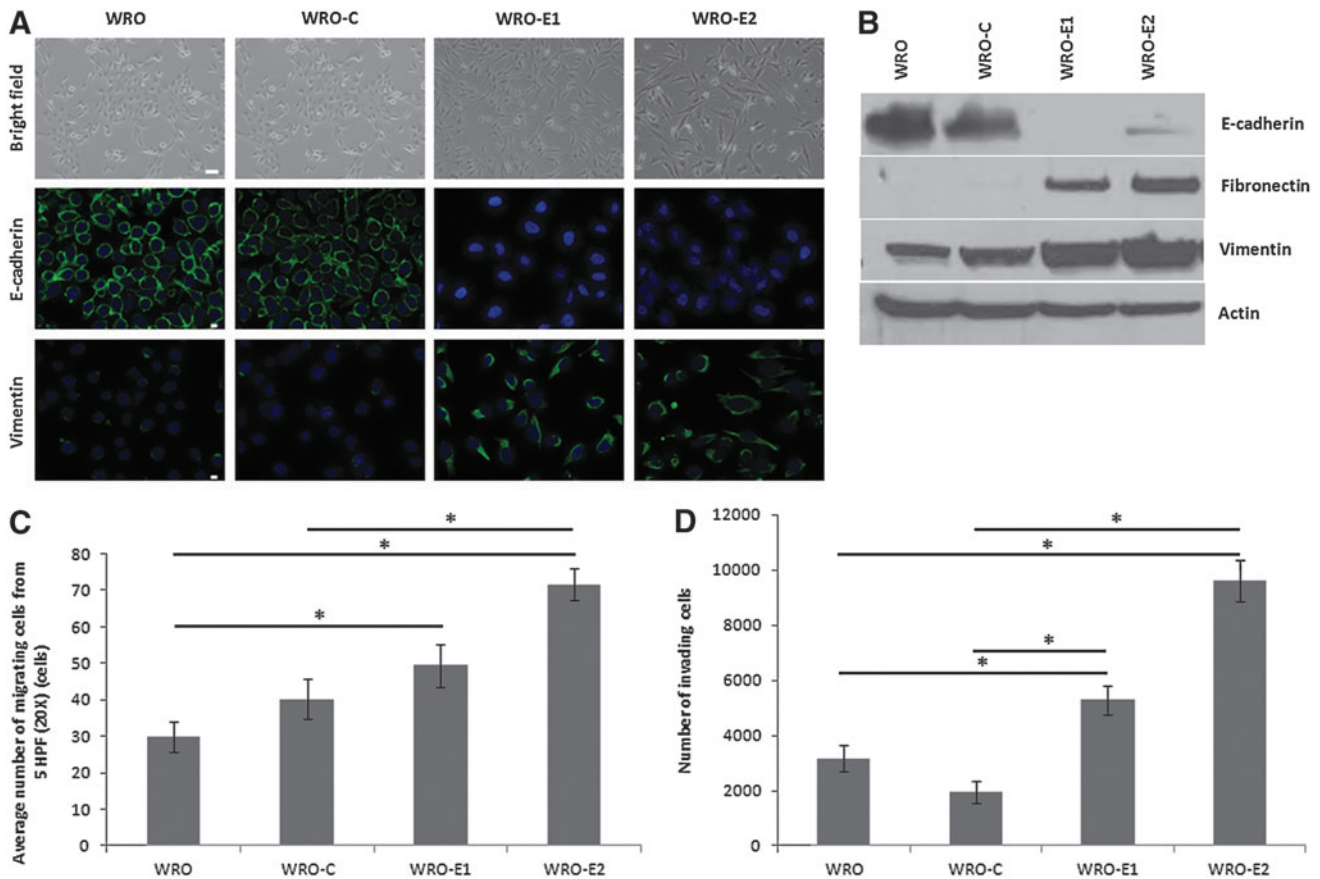


**FIG. 1.** Stable E-cadherin silencing induces epithelial–mesenchymal transition (EMT) in WRO82-1 thyroid cancer cells. (A) Stable short hairpin RNA (shRNA) repression of E-cadherin in WRO82-1 cells results in a transition to a mesenchymal morphology and the expression of vimentin in two clones (WRO-E1 and WRO-E2), as compared with parental cells (WRO) or control shRNA-transfected cells (WRO-C). Scale bars: (top) 25  $\mu\text{m}$ ; (middle and bottom) 10  $\mu\text{m}$ . (B) Western blot of WRO, WRO-C, WRO-E1, and WRO-E2 cells. (C and D) Quantification of (C) migrating and (D) invading cells, using a Boyden chamber invasion assay with 10% FCS used as a chemoattractant ( $*p < 0.05$ ,  $t$  test). HPF, high-power field.

$t$  test), but not WRO-C (Fig. 1C). For invasion assays, both WRO-E1 and WRO-E2 also showed significant increases in the number of invading cells as compared with either WRO or WRO-C (Fig. 1D;  $p < 0.01$ ,  $t$  test) after 20 hr, using 10% FCS as a chemoattractant.

#### *Herpesvirus attaches rapidly to the surface of WRO cells with EMT phenotype*

To directly visualize viral attachment to cell surfaces, we exposed WRO-E1, WRO-E2, WRO-C, and WRO to HSV-1 VP-16-GFP, a herpes simplex virus type 1 in which the viral envelope incorporates a GFP-tagged VP16 protein, making the virus directly visible. GFP signal was observed by time-lapse fluorescence microscopy. HSV-1 VP-16-GFP was detected rapidly accumulating on the cell surfaces of both WRO-E1 and WRO-E2 cells over a 6-hr period. In contrast, virus attached much less to the surfaces of WRO or WRO-C cells over the same interval (Fig. 2A).

#### *Herpesviral entry and gene expression is increased in WRO cells with EMT phenotype*

NV1066 and NV1023 are HSV-1 genetically modified to express GFP and  $\beta$ -galactosidase, respectively. The ex-

pression of these proteins after viral exposure indicates successful viral entry and early gene expression. Both WRO-E1 and WRO-E2 demonstrated increased susceptibility to herpesviral entry and early gene expression by the NV1066 virus as compared with WRO. GFP expression detected by fluorescence microscopy was significantly higher in both WRO-E1 and WRO-E2 on days 1 and 2 after infection as compared with WRO as control. WRO-C was not used as the control in these experiments because of its stable transfection by shRNA targeting GFP. GFP expression began to decrease on day 3 because of the induction of viral oncolytic cell death (Fig. 2B). In similar experiments,  $\beta$ -galactosidase gene expression was assessed by X-Gal staining after exposure of cell lines to the NV1023 virus. Both WRO-E1 and WRO-E2 showed significantly more intense and widespread X-Gal staining as compared with WRO and WRO-C (Fig. 2C).

We compared a time course of expression of herpesviral proteins to assess for alterations in HSV-1 sensitivity that may be induced by EMT. Immunoblots were performed of two early-expressing herpesviral proteins (ICP27 and ICP8) and one late-expressing protein (gC). ICP27 appeared as early as 6 hr after NV1023 infection in WRO-E1 and WRO-E2, whereas expression occurred at 12 hr in WRO and

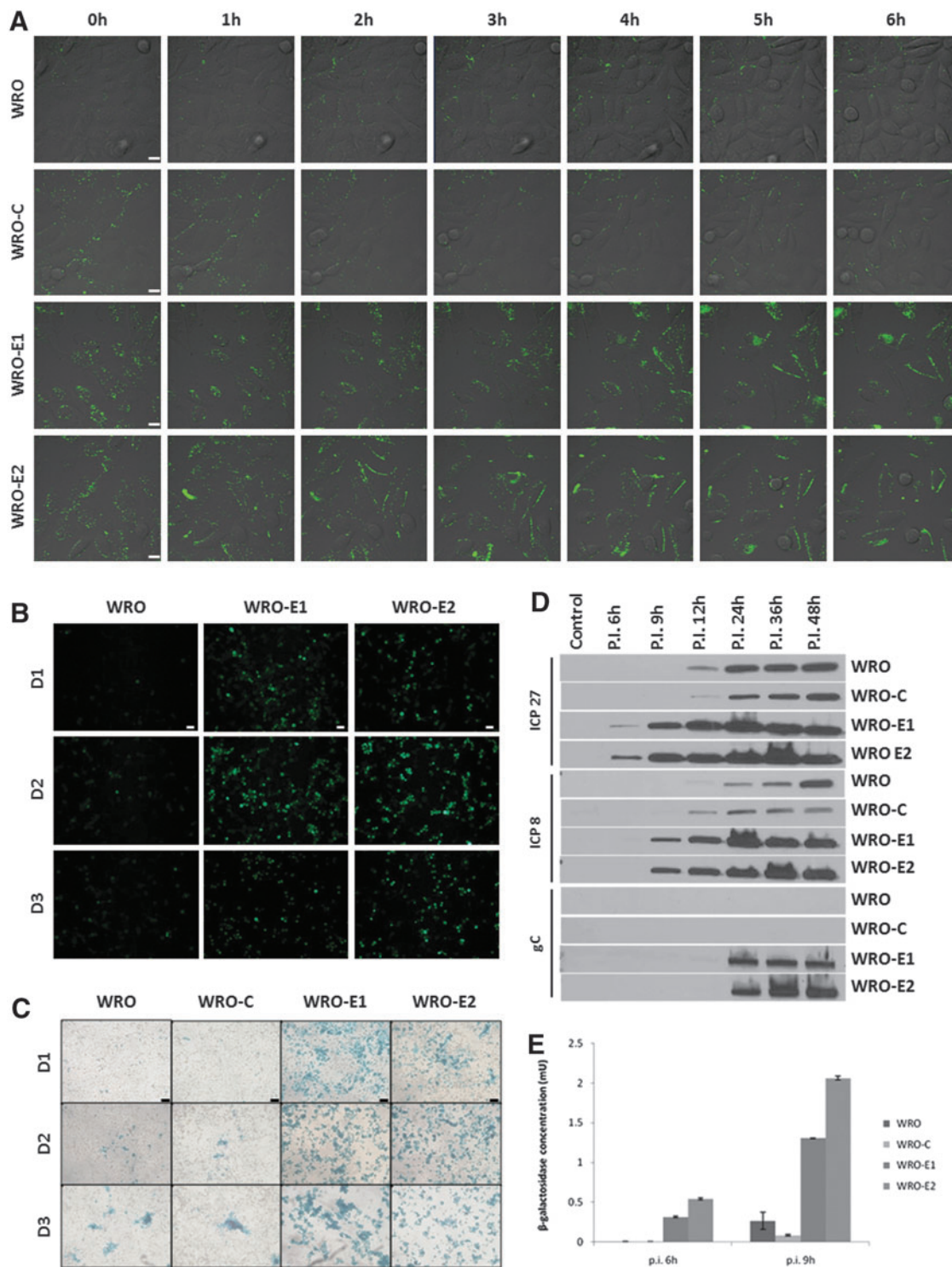


**FIG. 2.** WRO cells in EMT exhibit increased susceptibility to HSV-1 attachment, infection, and gene expression. **(A)** There is earlier and increased HSV-1 VP-16-GFP attachment to WRO-E1 and WRO-E2 cells (bottom rows) as compared with WRO and WRO-C cells (top rows), as visualized by time-lapse fluorescence microscopy. Scale bars: 10  $\mu$ m. **(B)** HSV-1 infection is enhanced in WRO-E1 and WRO-E2 as compared with WRO after infection with the herpesvirus NV1066 (MOI of 0.5), which expresses GFP. Scale bars: 25  $\mu$ m. **(C)** HSV-1 infection is enhanced in WRO-E1 and WRO-E2 as compared with WRO-C and WRO with the herpesvirus NV1023 (MOI of 0.5), which expresses  $\beta$ -galactosidase. Detected by X-Gal histochemical staining. Scale bars: 75  $\mu$ m. **(D)** A time course Western blot of the early herpesviral gene products ICP27 (top) and ICP8 (middle), and the late herpesviral gene product gC (bottom) in cells after infection with NV1023 (MOI of 1) over a 48-hr period shows earlier and more robust herpesviral gene expression by WRO-E1 and WRO-E2 as compared with control cells. **(E)** Quantification of viral  $\beta$ -galactosidase production by cells 6 and 9 hr after infection with the HSV-1 NV1023 (MOI of 5) demonstrates greater sensitivity of WRO-E1 and WRO-E2 to HSV-1 infection. p.i., postinfection. Color images available online at [www.liebertpub.com/hum](http://www.liebertpub.com/hum)

WRO-C. Similarly, ICP8 appeared in WRO-E1 and WRO-E2 at 9 hr postinfection, as compared with 12 hr in WRO and WRO-C at a lower level, reaching equivalent levels by 36 hr. The late viral protein gC was first detected in WRO-E1 and WRO-E2 at 24 hr of infection. In contrast, gC was not detected at 48 hr in WRO and WRO-C (Fig. 2D), although it is possible that gC would have been expressed at later time points. These results indicate that the temporal course of the sequence of HSV protein expression is significantly accelerated under EMT conditions as compared with control conditions.

To measure differences in cell line sensitivity to HSV-1 entry and early viral gene expression,  $\beta$ -galactosidase expression was quantified after exposure of each cell line to NV1023. At both 6 and 9 hr after exposure to NV1023, WRO-E1 and WRO-E2 showed significantly higher levels of  $\beta$ -galactosidase expression as compared with both WRO and WRO-C (Fig. 2E;  $p < 0.01$  for all comparisons between EMT and control cells,  $t$  test).

### EMT enhances nectin-1 expression, which is functional as an HSV-1 receptor

We hypothesized that EMT may alter nectin-1 expression and affect its function as an HSV-1 receptor. Immunofluorescence staining showed increased cytoplasmic and membranous nectin-1 expression in WRO-E1 and WRO-E2 as compared with WRO and WRO-C (Fig. 3A). Immunoblotting also demonstrated increased nectin-1 expression in WRO-E1 and WRO-E2 as compared with WRO and WRO-C (Fig. 3B).

To test whether the observed increased viral entry with EMT was mediated through nectin-1 as a viral receptor, we performed nectin-1 receptor-blocking assays as previously described (Huang *et al.*, 2007). After infection with NV1023,  $\beta$ -galactosidase expression was significantly higher in WRO-E1 and WRO-E2 as compared with WRO and WRO-C at both 6 and 9 hr after infection (Fig. 3C;  $p < 0.01$  for all comparisons,  $t$  test). The increase in  $\beta$ -galactosidase

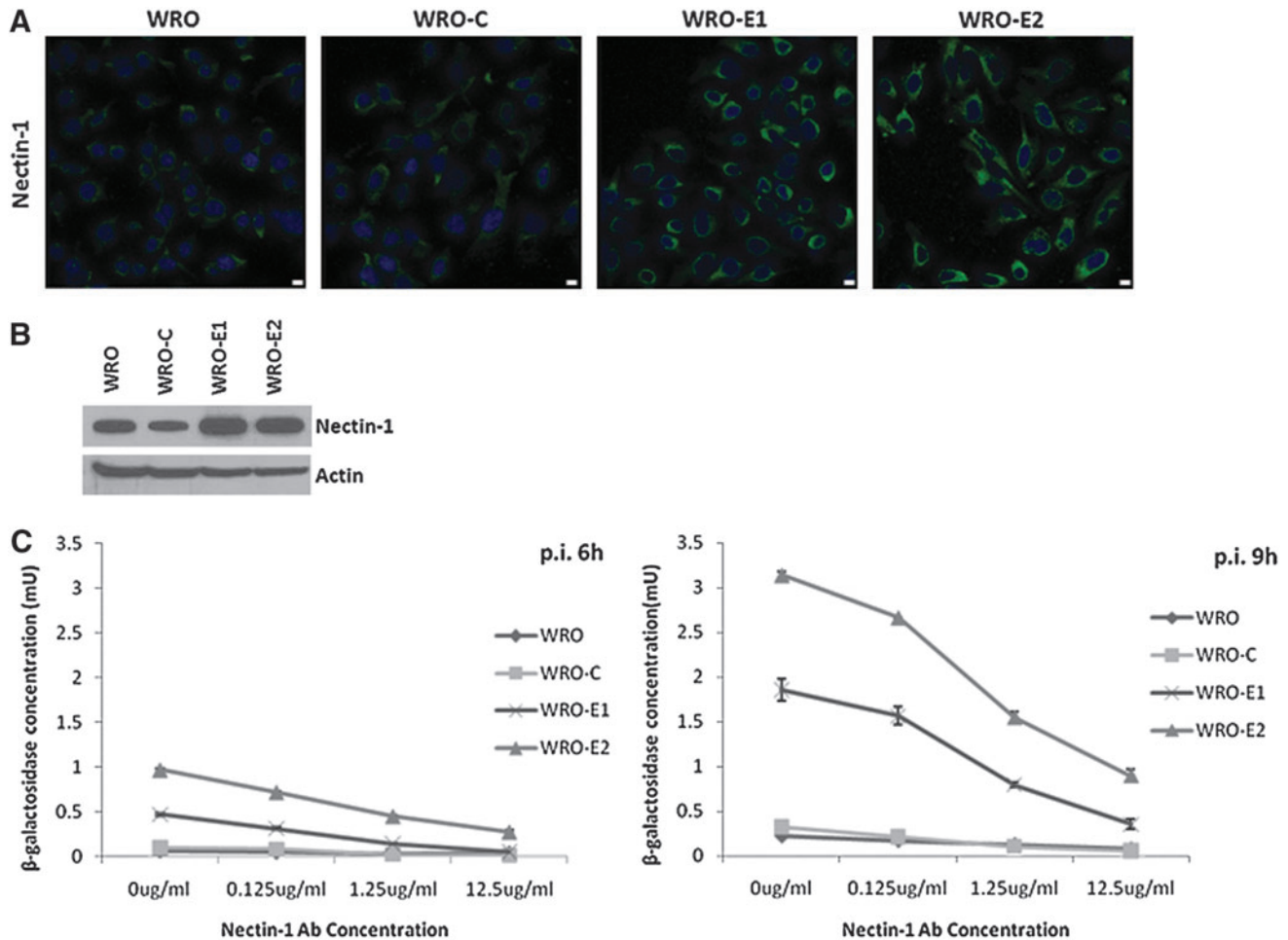


**FIG. 3.** Nectin-1 expression is enhanced in WRO cells with EMT as compared with controls, and is functional as a receptor for HSV-1. (A) Nectin-1 immunofluorescence microscopy shows enhanced nectin-1 expression in WRO-E1 and WRO-E2. Scale bars: 10  $\mu$ m. (B) Western blot for nectin-1 shows increased nectin-1 expression in WRO-E1 and WRO-E2. (C) Nectin-1 viral receptor-blocking assays show viral  $\beta$ -galactosidase production 6 and 9 hr after infection with the HSV-1 NV1023 (MOI of 5) in the presence of various concentrations of nectin-1 antibody. The enhanced viral entry into WRO-E1 and WRO-E2 cells is susceptible to receptor blockade with nectin-1 antibody. p.i., postinfection. Color images available online at [www.liebertpub.com/hum](http://www.liebertpub.com/hum)



expression for WRO-E1 and WRO-E2 was blocked in a dose-dependent fashion by increasing concentrations of nectin-1 antibody (Fig. 3C), suggesting that the predominant mechanism of enhanced viral entry was mediated through nectin-1.

#### *HSV-1 colocalization with nectin-1 is enhanced in WRO cells with EMT phenotype*

To directly visualize HSV-1 interactions with nectin-1, we generated a WRO82-1 cell line expressing nectin-1 tagged with tdTomato fluorescent protein, and then subsequently transfected shRNA targeting E-cadherin or control. WRO-Nectin-1-tdTomato-shEcad demonstrated diminished E-cadherin and enhanced cell surface nectin-1 tdTomato signal as compared with the WRO-Nectin-1-tdTomato-shControl, by fluorescence microscopy; signal intensity was quantified with MetaMorph (Fig. 4A and B;  $*p < 0.01$ ).

We exposed WRO-Nectin-1-tdTomato-shEcad or WRO-Nectin-1-tdTomato-shControl to HSV-1 expressing VP-16-GFP, which allows for the direct visualization of green viral particles. GFP and tdTomato fluorescent signals were then imaged by time-lapse fluorescence microscopy. HSV-1 VP-

16-GFP accumulated more on the cell surfaces of shEcad cells as compared with shControl cells over a 5-hr period (Fig. 4C). Colocalization of GFP and tdTomato fluorescence signal was determined by Metamorph software analysis. Colocalization of HSV-1 VP-16-GFP and Nectin-1-tdTomato was enhanced in shEcad as compared with shControl, indicating increased HSV-1 binding to this receptor in the EMT state (Fig. 4D).

#### *TGF- $\beta$ -mediated induction of EMT increases susceptibility to HSV-1 infection*

To determine whether our observations of increased HSV-1 susceptibility with EMT were specific to E-cadherin repression, we explored an alternative model of EMT induction resulting from TGF- $\beta$  stimulation. Panc-1 cells under exposure to TGF- $\beta$  gradually exhibit EMT, assuming a spindle shape morphology (Fig. 5A). Western blotting shows a loss of E-cadherin and gain of fibronectin with TGF- $\beta$  stimulation consistent with EMT. Panc-1 cells under TGF- $\beta$  stimulation also exhibit mildly increased levels of nectin-1 (Fig. 5B).

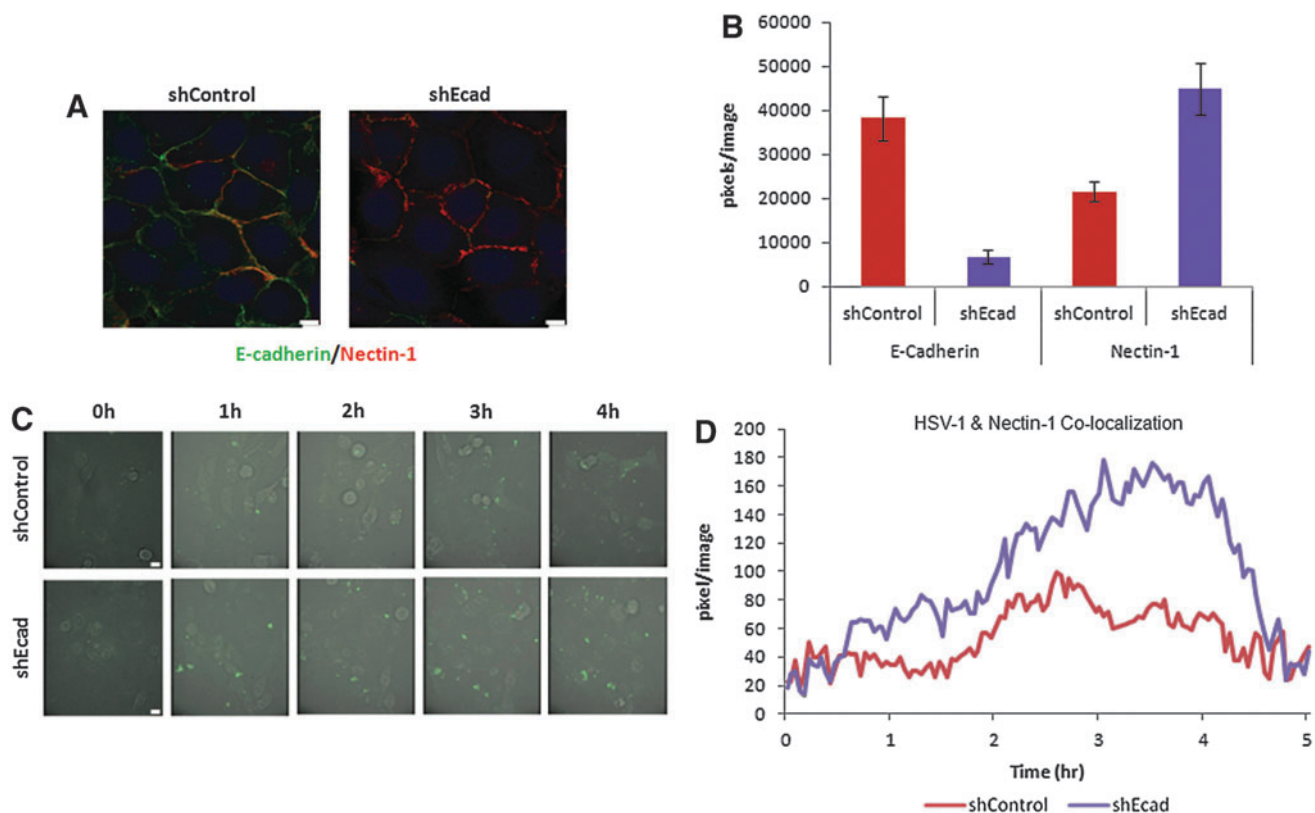


**FIG. 4.** HSV-1 colocalization with nectin-1 is enhanced in WRO cells with the EMT phenotype. (A) WRO cells were generated to express Nectin-1-td-tomato, and then transfected with shRNA silencing E-cadherin (WRO-Nectin-1-td-tomato-shEcad), or control (WRO-Nectin-1-td-tomato-shControl). Immunofluorescence microscopy demonstrates nectin-1 (red) and E-cadherin (green) expression in these cells. Scale bars: 10  $\mu$ m. (B) Image fluorescence quantification shows a reduction of E-cadherin and an increase in nectin-1 expression in WRO-Nectin-1-td-tomato-shEcad as compared with WRO-Nectin-1-td-tomato-shControl. (C) Time-lapse immunofluorescence microscopy shows that HSV-1 VP-16-GFP exhibits earlier and more robust attachment to WRO-Nectin-1-td-tomato-shEcad cells as compared with WRO-Nectin-1-td-tomato-shControl cells. Scale bars: 10  $\mu$ m. (D) The colocalization of HSV-1 VP-16-GFP (green) with nectin-1 (red) was measured and quantified by Metamorph software analysis of time-lapse immunofluorescence microscopy over a 5-hr period. There is enhanced colocalization of HSV-1 with nectin-1 in the WRO-Nectin-1-td-tomato-shEcad cells as compared with WRO-Nectin-1-td-tomato-shControl cells.

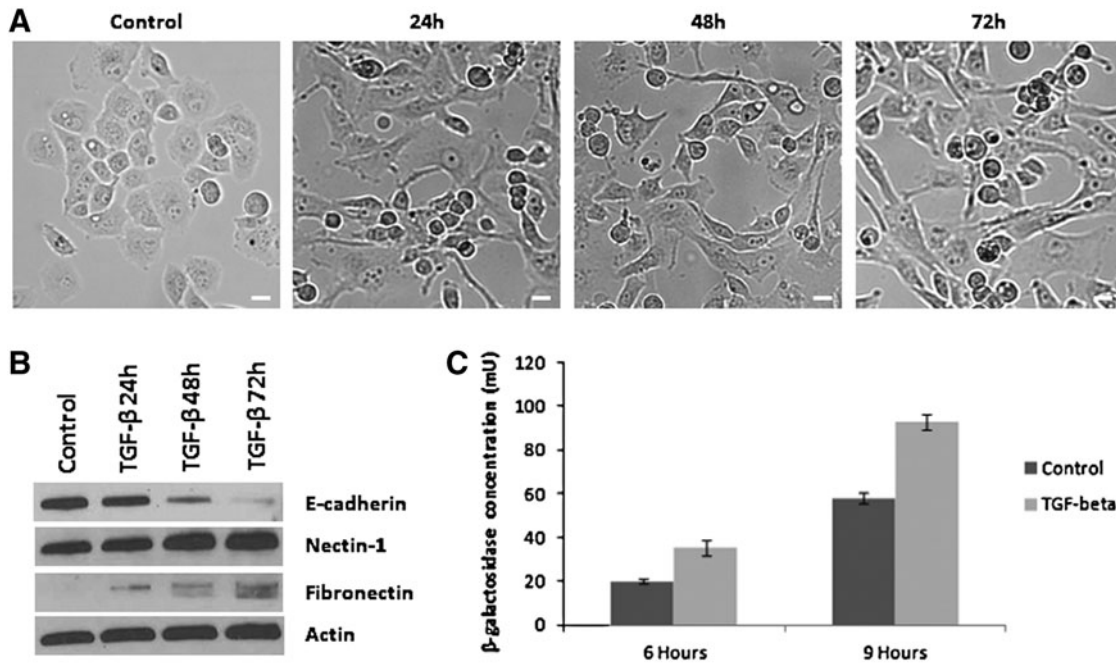


**FIG. 5.** TGF- $\beta$ -mediated induction of EMT increases susceptibility to HSV-1 infection. (A) TGF- $\beta$  induces morphologic changes of EMT in Panc-1 cells over 72 hr. Scale bars: 25  $\mu$ m. (B) Western blot demonstrates repression of E-cadherin, expression of fibronectin, and a mild increase in nectin-1 in Panc-1 cells treated with TGF- $\beta$ . (C) Panc-1 cells treated with TGF- $\beta$  for 48 hr were exposed to HSV-1 NV1023 at an MOI of 5.  $\beta$ -Galactosidase levels were quantified 6 and 9 hr after infection, and demonstrate enhanced susceptibility to HSV-1 by Panc-1 cells undergoing TGF- $\beta$ -induced EMT.

HSV-1 viral entry assays were performed by quantifying  $\beta$ -galactosidase expression after exposure to NV1023. Panc-1 cells under TGF- $\beta$  stimulation for 48 hr demonstrated significantly enhanced viral entry and  $\beta$ -galactosidase expression at both 6 and 9 hr after infection as compared with control, unstimulated Panc-1 cells (Fig. 5C;  $p < 0.01$ ,  $t$  test).

#### EMT increases susceptibility to herpesviral cytotoxicity and replication

Cell viability assays were used to assess the sensitivity of cell lines to HSV-1-induced cytotoxicity. Cell lines were exposed to NV1023 at MOIs of 0.5 and 1. Both WRO and WRO-C were insensitive to NV1023 at these doses for 7 days after exposure and remained fully viable. In contrast, both WRO-E1 and WRO-E2 showed significant sensitivity to viral cytotoxicity at these doses, reaching greater than 80% cell death for both MOIs by day 7 ( $p < 0.05$  on days

2–7,  $t$  test, for WRO-E1 or WRO-E2 as compared with WRO or WRO-C) (Fig. 6A).

The ability of NV1023 to replicate within these cell lines was assessed by viral plaque assays performed 48 hr after viral exposure at an MOI of 1. WRO-E1 and WRO-E2 supported significantly greater viral replication as compared with WRO and WRO-C ( $p < 0.01$ ) (Fig. 6B).

Because the cell proliferation rate may affect the viral proliferation rate, we compared cell proliferation across the various cell lines. There were no significant differences between the WRO-E1 and WRO-E2 cell lines and WRO, although WRO-C did proliferate slightly faster than the other cell lines ( $*p < 0.05$  on days 4–7,  $t$  test) (Fig. 6C).

#### EMT tumors are more susceptible than non-EMT tumors to HSV-1 therapy in vivo

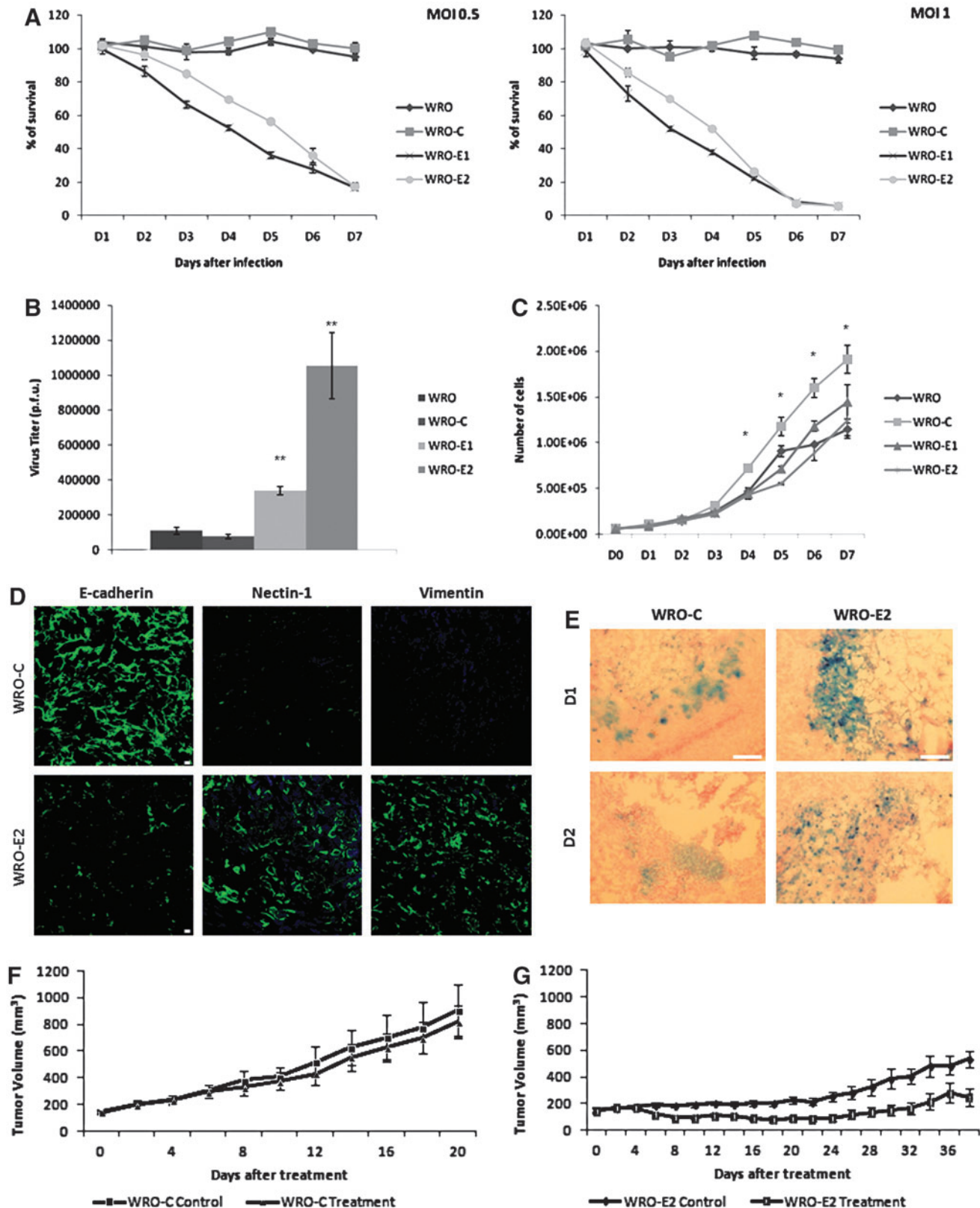
Tumors were generated in the flanks of athymic nude mice by subcutaneous injection of WRO-E2 and WRO-C

**FIG. 6.** EMT increases cancer cell susceptibility to herpesviral cytotoxicity and replication both *in vitro* and *in vivo*. (A) One-week cytotoxicity assays were performed after exposure of cells to HSV-1 NV1023 at MOIs of 0.5 (left) and 1 (right). WRO-E1 and WRO-E2 exhibited significantly enhanced sensitivity to viral cytotoxicity. (B) Viral replication assays were performed 2 days after exposure of cells to NV1023 at an MOI of 1. WRO-E1 and WRO-E2 supported significantly enhanced viral replication (\*\* $p < 0.01$ , for comparisons with either WRO or WRO-C,  $t$  test). (C) Cell proliferation rates of WRO-E1 and WRO-E2 do not account for enhanced viral sensitivity by WRO-E1 and WRO-E2, because their proliferation was either equivalent to or slower than that of controls ( $*p < 0.05$ ). (D) Murine flank tumors arising from WRO-C and WRO-E2 cell lines were excised for immunofluorescence microscopy of E-cadherin, nectin-1, and vimentin to demonstrate the maintenance of an EMT expression profile in established tumors. Scale bars: 25  $\mu$ m. (E) Murine flank tumors from WRO-C and WRO-E2 were injected with a single intratumoral dose of HSV-1 NV1023, and then excised for X-Gal staining on days 1 and 2 to assess for degree of viral infection in tumor tissue. Scale bars: 200  $\mu$ m. (F) A single intratumoral injection of NV1023 fails to induce significant tumor volume regression of murine WRO-C flank tumors. (G) A single intratumoral injection of NV1023 results in significant tumor regression of murine WRO-E2 flank tumors on day 6 after treatment and onward ( $p < 0.01$ ,  $t$  test). Color images available online at [www.liebertpub.com/hum](http://www.liebertpub.com/hum)



cells. Immunostaining of excised, untreated tumors demonstrated that WRO-C tumors retained intact E-cadherin expression, whereas established WRO-E2 tumors maintained repression of E-cadherin. WRO-E2 tumors also maintained significantly enhanced nectin-1 and vimentin

expression as compared with WRO-C tumors (Fig. 6D). We observed that shEcad-WRO flank tumors grew slower than shControl-WRO tumors; this finding is compatible with prior associations of EMT with decreased cellular proliferation rates, as cell morphological changes may be less



compatible with cell division, and programs inducing EMT may impair cell cycle progression (Floor *et al.*, 2011). Tumor volumes were therefore monitored for a longer time period (38 days) for WRO-E2 as compared with WRO-C (20 days).

Tumors were injected with a single dose of NV1023 ( $1 \times 10^7$  PFU) and excised on days 1 and 2 (Fig. 6E) for X-Gal staining to detect  $\beta$ -galactosidase expression. WRO-E2 tumors exhibited more widespread and intense X-Gal staining as compared with WRO-C tumors, demonstrating enhanced susceptibility to HSV-1 infection.

Tumor volumes were monitored longitudinally after a single intratumoral injection of  $1 \times 10^7$  PFU of NV1023. This dose of NV1023 had no significant effect on impeding the growth in WRO-C tumors (Fig. 6F). In contrast, a single intratumoral injection of NV1023 significantly inhibited tumor volume progression in WRO-E2 tumors (Fig. 6G) ( $p < 0.01$ , on day 6 after treatment and onward, *t* test).

There were no toxic side effects noticed related to viral therapy in any of the animals, and mean animal body weights remained stable in all experimental groups.

## Discussion

The transition of an epithelial carcinoma to a mesenchymal phenotype (epithelial-to-mesenchymal transition, or EMT) is characterized by the loss of cell adhesion, cell detachment from neighboring cells, and enhanced ability to migrate through extracellular matrix (Yang and Weinberg, 2008; Floor *et al.*, 2011). This process in cancer progression shares similarities with the EMT that also occurs during development and wound healing. EMT may be induced by signals (including TGF- $\beta$ ) arising from tumor-associated stroma, which then lead to the induction of a variety of transcription factors (including Snail, Slug, ZEB1, Twist, Goosecoid, FOXC2) to initiate an EMT program (Kalluri and Weinberg, 2009). A hallmark of EMT is the loss of cell-cell adherens junctions and the loss of E-cadherin expression (Yang and Weinberg, 2008). EMT typically occurs at the invasive front of cancers, and is an independent indicator of poor prognosis. EMT enhances cancer cell invasive and metastatic abilities, and also may inhibit apoptosis and induce stem cell properties. The need to develop therapeutic approaches that may target EMT was highlighted as a research priority at a special conference at the American Association for Cancer Research (Roussos *et al.*, 2010).

Unfortunately, cancer cells undergoing EMT are poor targets for gene or viral therapy using adenoviruses and coxsackieviruses. Lacher and colleagues showed that TGF- $\beta$ -mediated induction of EMT inhibits cell surface coxsackievirus and adenovirus receptor (CAR) expression, and repression of the TGF- $\beta$  pathway leads to reexpression of CAR (Lacher *et al.*, 2006). Similar findings have been demonstrated for Raf/MAPK (mitogen-activated protein kinase) pathway induction and a loss of CAR expression on cancer cells (Anders *et al.*, 2003). These findings explain why carcinomas with EMT characteristics are poorly responsive to adenovirus-mediated therapy, and highlight a need to identify alternative therapeutic approaches for these aggressive malignancies.

Herpes oncolytic viral therapy harnesses the natural infectious and lytic ability of a replication-competent virus

toward the goal of treating malignant tumors. Genetically modified HSV-1 have been developed that exhibit an ability to infect and induce regression of tumors in experimental models. These viruses have been attenuated to enhance safety for clinical application, and also to favor selective viral replication within rapidly dividing host cells (Toda *et al.*, 1998; Kooby *et al.*, 1999; Toyozumi *et al.*, 1999; Walker *et al.*, 1999; Coukos *et al.*, 2000; McAuliffe *et al.*, 2000; Wong *et al.*, 2001a, 2010; Yu *et al.*, 2004). Genetic deletions engineered into some herpesviruses might allow for preferential viral replication within Ras-activated cells (Farassati *et al.*, 2001) or MEK (MAPK/ERK [extracellular signal-regulated kinase] kinase)-activated cells (Smith *et al.*, 2006).

The ability of HSV-1 to successfully enter a cell is dependent on the presence of specific cell surface receptors. During HSV-1 entry, an HSV-1 virion is initially attracted to a cell surface through electrostatic interactions between envelope glycoproteins B and C (gB and gC) and ubiquitous cell surface heparan sulfate proteoglycans (Spear and Longnecker, 2003). Next, critical interactions must occur between HSV-1 envelope glycoprotein D (gD) and one of three essential cell membrane receptors: nectin-1, herpesvirus entry mediator (HVEM), or 3-O-sulfated heparan sulfate (Montgomery *et al.*, 1996; Geraghty *et al.*, 1998; Spear and Longnecker, 2003). Viral proteins gH and gL subsequently mediate fusion of the viral envelope with the cell membrane and complete viral entry. A key step in determining successful HSV-1 entry is the interaction of viral envelope gD with one of the three cell surface receptors (Spear and Longnecker, 2003; Krummenacher *et al.*, 2004). Our laboratory has repeatedly shown previously that the susceptibility of a cancer to oncolytic HSV-1 correlates with its expression level of the gD receptor nectin-1 (Huang *et al.*, 2007; Yu *et al.*, 2007a, 2008). The quantity of cell surface nectin-1 is predictive of the susceptibility of the cell to HSV-1 entry, gene expression, viral replication, cytotoxicity, and the degree of tumor regression seen *in vivo* after HSV-1 therapy (Huang *et al.*, 2007; Yu *et al.*, 2007a). This concept has been demonstrated to be applicable for HSV-1 therapy of thyroid cancer (Huang *et al.*, 2007), squamous cell carcinoma (Yu *et al.*, 2007a), and more recently even lymphoproliferative disease (Wang *et al.*, 2012). Furthermore, we have demonstrated that antibody studies blocking the nectin-1 receptor, and conversely forced overexpression of nectin-1, both lead to the according functional changes in cell susceptibility to HSV-1 infection, for both squamous cell carcinomas and thyroid cancers (Huang *et al.*, 2007; Yu *et al.*, 2007a).

Importantly, nectin-1 normally functions as an intercellular adhesion molecule. Nectin-1 forms dimers that bridge across epithelial cells as part of intercellular adherens junctions (AJs) (Takai *et al.*, 2003). Another key component of AJs is dimers formed by E-cadherin. AJs and other junctions, such as tight junctions and desmosomes, maintain the organization, polarity, and cell-cell contacts between normal epithelial cells (Perez-Moreno *et al.*, 2003). Nectin-1 therefore serves in a unique, dual role as (1) a critical HSV-1 gD receptor and (2) a key structural component of cell-cell AJs.

Nectin-1 that is normally engaged in intact AJs is relatively inaccessible to serve as an HSV-1 receptor (Yoon

and Spear, 2002). However, the disruption of AJs under low calcium conditions releases the engaged nectin-1 to serve as a functional receptor for HSV-1 (Yoon and Spear, 2002). This nectin-1 release increases cell susceptibility to HSV-1 infection, and may also enhance the efficacy of herpes oncolytic viral therapy of cancer (Yu *et al.*, 2007b). AJs are also disrupted in the process of EMT. Although E-cadherin repression is a hallmark of EMT, the fate of nectin-1 during EMT is unclear. The process of EMT is particularly relevant to cancer therapy because cancers exhibiting EMT typically demonstrate more aggressive invasive and metastatic phenotypes, and worse clinical outcomes. We also demonstrated that the serial selection of cancer cells with increased invasive and migratory abilities (Yu *et al.*, 2005) or with increased nodal metastatic ability (Yu *et al.*, 2008) exhibited increased nectin-1 expression. On this basis, we hypothesized that cell surface nectin-1 expression might be increased after EMT, and we sought to explore relationships between EMT, nectin-1 expression, and HSV-1 sensitivity.

We induced EMT in a thyroid cancer cell line with an epithelial phenotype to generate two stable clones that exhibited enhanced migratory and invasive abilities. EMT significantly enhanced cancer sensitivity to HSV-1 through increased nectin-1 expression. Total nectin-1 protein levels increased mildly as determined by Western blotting, while cell surface nectin-1 appeared more significantly enhanced as detected by immunofluorescence (IF) microscopy. The greater detection of nectin-1 by IF microscopy might reflect a combination of both increased protein expression plus a release of preexisting nectin-1 normally engaged in adherens junctions that have become disrupted with EMT. Interestingly, one study has shown that nectin-1 may be detected at a higher level of expression on human metastatic thyroid cancer tissue as compared with normal or follicular adenoma thyroid tissue (Jensen *et al.*, 2010), supporting a concept of increasing nectin-1 expression with oncogenicity in thyroid cancer.

The induction of EMT leads to an increase in HSV-1 binding to cancer cell surfaces. Receptor-blocking studies revealed that nectin-1 was the main receptor through which increased infection was occurring, and virus-receptor colocalization studies provide direct evidence of enhanced HSV-1 attachment to nectin-1 in EMT cells. Herpesviral entry, protein production, downstream signaling, and cytotoxicity were all enhanced in EMT cells as compared with control cells. Importantly, these effects translate *in vivo* to enhanced viral infection and tumor regression of EMT flank tumors as compared with control flank tumors in mice after a single intratumoral injection of HSV-1.

These findings suggest that cancer cells in an EMT state are naturally more susceptible targets for herpesviral therapy. It is likely that herpesviral vectors used for gene transfer, such as herpes amplicons, may also show similar advantages as herpes oncolytic viruses for targeting EMT cells. This strategy might theoretically be applicable for any therapeutic vector engineered to use glycoprotein D as a mechanism of gaining entry into a cell. These findings conceptually demonstrate that the process of EMT itself can be targeted by the identification of a cell surface protein enhanced in the EMT state, which can then be exploited for therapeutic gain.

EMT induces an invasive and metastatic phenotype, and heralds aggressive disease with worse clinical outcomes despite conventional therapies. Patients with malignancies exhibiting EMT are among those in need of novel and effective therapies with a different mechanism of activity. Therefore, the application of novel therapeutic approaches using gD to target nectin-1-expressing cells in an EMT state may be of significant potential future clinical value.

### Acknowledgments

The authors thank their laboratory colleagues for providing insight, Dr. Miho Shimada (Rockefeller University) for helping to construct pEF1 $\alpha$ -Nectin-1-tdTomato, and Dr. Sho Fujisawa and the Molecular Cytology Core Facility at MSKCC for assistance with time-lapse immunofluorescence microscopy.

### Author Disclosure Statement

The authors (C.H.C., W.Y.C., S.F.L., R.J.W.) declare that they each have no conflict of interest with any part of this study. This work was funded by NIH grant R21DE19015.

### References

- Anders, M., Christian, C., McMahon, M., *et al.* (2003). Inhibition of the Raf/MEK/ERK pathway up-regulates expression of the coxsackievirus and adenovirus receptor in cancer cells. *Cancer Res.* 63, 2088–2095.
- Bennett, J.J., Malhotra, S., Wong, R.J., *et al.* (2001). Interleukin 12 secretion enhances antitumor efficacy of oncolytic herpes simplex viral therapy for colorectal cancer. *Ann. Surg.* 233, 819–826.
- Coukos, G., Makrigiannakis, A., Kang, E.H., *et al.* (2000). Oncolytic herpes simplex virus-1 lacking ICP34.5 induces p53-independent death and is efficacious against chemotherapy-resistant ovarian cancer. *Clin. Cancer Res.* 6, 3342–3353.
- Eisenberg, D.P., Adusumilli, P.S., Hendershott, K.J., *et al.* (2005). 5-Fluorouracil and gemcitabine potentiate the efficacy of oncolytic herpes viral gene therapy in the treatment of pancreatic cancer. *J. Gastrointest. Surg.* 9, 1068–1077; discussion 1077–1069.
- Ellenrieder, V., Hendler, S.F., Boeck, W., *et al.* (2001). Transforming growth factor  $\beta_1$  treatment leads to an epithelial–mesenchymal transdifferentiation of pancreatic cancer cells requiring extracellular signal-regulated kinase 2 activation. *Cancer Res.* 61, 4222–4228.
- Farassati, F., Yang, A.D., and Lee, P.W. (2001). Oncogenes in Ras signalling pathway dictate host-cell permissiveness to herpes simplex virus 1. *Nat. Cell Biol.* 3, 745–750.
- Fidler, I.J. (2003). The pathogenesis of cancer metastasis: The “seed and soil” hypothesis revisited. *Nat. Rev. Cancer* 3, 453–458.
- Floor, S., van Staveren, W.C., Larsimont, D., *et al.* (2011). Cancer cells in epithelial-to-mesenchymal transition and tumor-propagating-cancer stem cells: Distinct, overlapping or same populations. *Oncogene* 30, 4609–4621.
- Geraghty, R.J., Krummenacher, C., Cohen, G.H., *et al.* (1998). Entry of alphaherpesviruses mediated by poliovirus receptor-related protein 1 and poliovirus receptor. *Science* 280, 1618–1620.
- Gil, Z., Rein, A., Brader, P., *et al.* (2007). Nerve-sparing therapy with oncolytic herpes virus for cancers with neural invasion. *Clin. Cancer Res.* 13, 6479–6485.



- Huang, Y.Y., Yu, Z., Lin, S.F., *et al.* (2007). Nectin-1 is a marker of thyroid cancer sensitivity to herpes oncolytic therapy. *J. Clin. Endocrinol. Metab.* 92, 1965–1970.
- Hugo, H., Ackland, M.L., Blick, T., *et al.* (2007). Epithelial–mesenchymal and mesenchymal–epithelial transitions in carcinoma progression. *J. Cell. Physiol.* 213, 374–383.
- Jensen, K., Patel, A., Larin, A., *et al.* (2010). Human herpes simplex viruses in benign and malignant thyroid tumours. *J. Pathol.* 221, 193–200.
- Kalluri, R., and Weinberg, R.A. (2009). The basics of epithelial–mesenchymal transition. *J. Clin. Invest.* 119, 1420–1428. [Published erratum appears in *J. Clin. Invest.* 2010;120:1786.]
- Kooby, D.A., Carew, J.F., Halterman, M.W., *et al.* (1999). Oncolytic viral therapy for human colorectal cancer and liver metastases using a multi-mutated herpes simplex virus type-1 (G207). *FASEB J.* 13, 1325–1334.
- Krummenacher, C., Baribaud, F., Ponce de Leon, M., *et al.* (2004). Comparative usage of herpesvirus entry mediator A and nectin-1 by laboratory strains and clinical isolates of herpes simplex virus. *Virology* 322, 286–299.
- Kurrey, N.K., Jalgaonkar, S.P., Joglekar, A.V., *et al.* (2009). Snail and slug mediate radioresistance and chemoresistance by antagonizing p53-mediated apoptosis and acquiring a stem-like phenotype in ovarian cancer cells. *Stem Cells* 27, 2059–2068.
- La Boissière, S., Izeta, A., Malcomber, S., and O’Hare, P. (2004). Compartmentalization of VP16 in cells infected with recombinant herpes simplex virus expressing VP16-green fluorescent protein fusion proteins. *J. Virol.* 78, 8002–8014.
- Lacher, M.D., Tiirikainen, M.I., Saunier, E.F., *et al.* (2006). Transforming growth factor- $\beta$  receptor inhibition enhances adenoviral infectability of carcinoma cells via up-regulation of coxsackie and adenovirus receptor in conjunction with reversal of epithelial–mesenchymal transition. *Cancer Res.* 66, 1648–1657.
- Lin, S.F., Price, D.L., Chen, C.H., *et al.* (2008). Oncolytic vaccinia virotherapy of anaplastic thyroid cancer *in vivo*. *J. Clin. Endocrinol. Metab.* 93, 4403–4407.
- McAuliffe, P.F., Jarnagin, W.R., Johnson, P., *et al.* (2000). Effective treatment of pancreatic tumors with two multi-mutated herpes simplex oncolytic viruses. *J. Gastrointest. Surg.* 4, 580–588.
- Mineta, T., Rabkin, S.D., Yazaki, T., *et al.* (1995). Attenuated multi-mutated herpes simplex virus-1 for the treatment of malignant gliomas. *Nat. Med.* 1, 938–943.
- Montgomery, R.I., Warner, M.S., Lum, B.J., and Spear, P.G. (1996). Herpes simplex virus-1 entry into cells mediated by a novel member of the TNF/NGF receptor family. *Cell* 87, 427–436.
- Onder, T.T., Gupta, P.B., Mani, S.A., *et al.* (2008). Loss of E-cadherin promotes metastasis via multiple downstream transcriptional pathways. *Cancer Res.* 68, 3645–3654.
- Peng, K.W., TenEyck, C.J., Galanis, E., *et al.* (2002). Intraperitoneal therapy of ovarian cancer using an engineered measles virus. *Cancer Res.* 62, 4656–4662.
- Perez-Moreno, M., Jamora, C., and Fuchs, E. (2003). Sticky business: Orchestrating cellular signals at adherens junctions. *Cell* 112, 535–548.
- Polyak, K., and Weinberg, R.A. (2009). Transitions between epithelial and mesenchymal states: Acquisition of malignant and stem cell traits. *Nat. Rev. Cancer* 9, 265–273.
- Reid, V., Yu, Z., Schuman, T., *et al.* (2008). Herpes oncolytic therapy of salivary gland carcinomas. *Int. J. Cancer* 122, 202–208.
- Roussos, E.T., Keckesova, Z., Haley, J.D., *et al.* (2010). AACR special conference on epithelial–mesenchymal transition and cancer progression and treatment. *Cancer Res.* 70, 7360–7364.
- Shah, A.N., Summy, J.M., Zhang, J., *et al.* (2007). Development and characterization of gemcitabine-resistant pancreatic tumor cells. *Ann. Surg. Oncol.* 14, 3629–3637.
- Smith, K.D., Mezhir, J.J., Bickenbach, K., *et al.* (2006). Activated MEK suppresses activation of PKR and enables efficient replication and *in vivo* oncolysis by  $\Delta\gamma_{134.5}$  mutants of herpes simplex virus 1. *J. Virol.* 80, 1110–1120.
- Spear, P.G., and Longnecker, R. (2003). Herpesvirus entry: An update. *J. Virol.* 77, 10179–10185.
- Stanziale, S.F., Petrowsky, H., Adusumilli, P.S., *et al.* (2004). Infection with oncolytic herpes simplex virus-1 induces apoptosis in neighboring human cancer cells: A potential target to increase anticancer activity. *Clin. Cancer Res.* 10, 3225–3232.
- Stewart, S.A., Dykxhoorn, D.M., Palliser, D., *et al.* (2003). Lentivirus-delivered stable gene silencing by RNAi in primary cells. *RNA* 9, 493–501.
- Takai, Y., Irie, K., Shimizu, K., *et al.* (2003). Nectins and nectin-like molecules: Roles in cell adhesion, migration, and polarization. *Cancer Sci.* 94, 655–667.
- Thiery, J.P., Acloque, H., Huang, R.Y., and Nieto, M.A. (2009). Epithelial–mesenchymal transitions in development and disease. *Cell* 139, 871–890.
- Thompson, E.W., Newgreen, D.F., and Tarin, D. (2005). Carcinoma invasion and metastasis: A role for epithelial–mesenchymal transition? *Cancer Res.* 65, 5991–5995; discussion 5995.
- Toda, M., Rabkin, S.D., and Martuza, R.L. (1998). Treatment of human breast cancer in a brain metastatic model by G207, a replication-competent multimitated herpes simplex virus 1. *Hum. Gene Ther.* 9, 2177–2185.
- Toyoizumi, T., Mick, R., Abbas, A.E., *et al.* (1999). Combined therapy with chemotherapeutic agents and herpes simplex virus type 1 ICP34.5 mutant (HSV-1716) in human non-small cell lung cancer. *Hum. Gene Ther.* 10, 3013–3029.
- Walker, J.R., McGeagh, K.G., Sundaresan, P., *et al.* (1999). Local and systemic therapy of human prostate adenocarcinoma with the conditionally replicating herpes simplex virus vector G207. *Hum. Gene Ther.* 10, 2237–2243.
- Wang, P.Y., Currier, M.A., Hansford, L., *et al.* (2012). Expression of HSV-1 receptors in EBV-associated lymphoproliferative disease determines susceptibility to oncolytic HSV. *Gene Ther.* 20, 761–769.
- Wong, J., Kelly, K., Mittra, A., *et al.* (2010). A third-generation herpesvirus is effective against gastroesophageal cancer. *J. Surg. Res.* 163, 214–220.
- Wong, R.J., Kim, S.H., Joe, J.K., *et al.* (2001a). Effective treatment of head and neck squamous cell carcinoma by an oncolytic herpes simplex virus. *J. Am. Coll. Surg.* 193, 12–21.
- Wong, R.J., Patel, S.G., Kim, S., *et al.* (2001b). Cytokine gene transfer enhances herpes oncolytic therapy in murine squamous cell carcinoma. *Hum. Gene Ther.* 12, 253–265.
- Wong, R.J., Joe, J.K., Kim, S.H., *et al.* (2002). Oncolytic herpesvirus effectively treats murine squamous cell carcinoma and spreads by natural lymphatics to treat sites of lymphatic metastases. *Hum. Gene Ther.* 13, 1213–1223.
- Wong, R.J., Chan, M.K., Yu, Z., *et al.* (2004). Effective intravenous therapy of murine pulmonary metastases with an

- oncolytic herpes virus expressing interleukin 12. *Clin. Cancer Res.* 10, 251–259.
- Yang, A.D., Fan, F., Camp, E.R., *et al.* (2006). Chronic oxaliplatin resistance induces epithelial-to-mesenchymal transition in colorectal cancer cell lines. *Clin. Cancer Res.* 12, 4147–4153.
- Yang, J., and Weinberg, R.A. (2008). Epithelial–mesenchymal transition: At the crossroads of development and tumor metastasis. *Dev. Cell* 14, 818–829.
- Yoon, M., and Spear, P.G. (2002). Disruption of adherens junctions liberates nectin-1 to serve as receptor for herpes simplex virus and pseudorabies virus entry. *J. Virol.* 76, 7203–7208.
- Yu, Z., Eisenberg, D.P., Singh, B., *et al.* (2004). Treatment of aggressive thyroid cancer with an oncolytic herpes virus. *Int. J. Cancer* 112, 525–532.
- Yu, Z., Chan, M.K., O-charoenrat, P., *et al.* (2005). Enhanced nectin-1 expression and herpes oncolytic sensitivity in highly migratory and invasive carcinoma. *Clin. Cancer Res.* 11, 4889–4897.
- Yu, Z., Adusumilli, P.S., Eisenberg, D.P., *et al.* (2007a). Nectin-1 expression by squamous cell carcinoma is a predictor of herpes oncolytic sensitivity. *Mol. Ther.* 15, 103–113.
- Yu, Z., Li, S., Huang, Y.Y., *et al.* (2007b). Calcium depletion enhances nectin-1 expression and herpes oncolytic therapy of squamous cell carcinoma. *Cancer Gene Ther.* 14, 738–747.
- Yu, Z., Li, S., Huang, Y.Y., *et al.* (2008). Sensitivity of squamous cell carcinoma lymph node metastases to herpes oncolytic therapy. *Clin. Cancer Res.* 14, 1897–1904.

Address correspondence to:

*Dr. Richard J. Wong*  
*Head and Neck Service, C-1069*  
*Department of Surgery*  
*Memorial Sloan-Kettering Cancer Center*  
*New York, NY 10021*

*E-mail:* wongr@mskcc.org

Received for publication September 13, 2013;  
accepted after revision February 21, 2014.

Published online: February 25, 2014.